

# Hepatocyte nuclear phenotype: the cross-talk between anabolic androgenic steroids and exercise in transgenic mice

Karina Fontana<sup>1,2</sup>, Marcela Aldrovani<sup>3</sup>, Flávia de Paoli<sup>3</sup>,  
Helena C. F. Oliveira<sup>4</sup>, Benedicto de Campos Vidal<sup>3</sup> and Maria Alice da Cruz-Höfling<sup>2</sup>

<sup>1</sup>Department of Pharmacology, Faculty of Medical Sciences, State University of Campinas (UNICAMP), Campinas, SP, Brazil,

<sup>2</sup>Department of Histology and Embryology, Institute of Biology, State University of Campinas (UNICAMP), Campinas, SP, Brazil,

<sup>3</sup>Department of Cell Biology, Institute of Biology, State University of Campinas (UNICAMP), Campinas, SP, Brazil and

<sup>4</sup>Department of Physiology and Biophysics, Institute of Biology, State University of Campinas (UNICAMP), Campinas, SP, Brazil

**Summary.** The growing and indiscriminate use of high doses of anabolic androgenic steroid (AAS) among youth and athletes has raised serious concerns about its hepatotoxic effects. Herein, the influence of AAS in the nuclear phenotype of hepatocytes was investigated in sedentary and trained mice heterozygous for the human CETP (cholesteryl ester transfer protein) transgene and for LDL-receptor null allele (CETP<sup>+/-</sup>LDLr<sup>+/-</sup>) by image analysis. Five groups were assayed comprising treadmill exercised (Ex) and sedentary (Sed) mice, administered mesterolone (AAS) or gum arabic (GA) and a sedentary blank control: G1(SedAAS), G2(SedGA), G3(ExAAS), G4(ExGA), and G5(SedBL). To assess nuclear phenotypes, the state of chromatin supraorganization, DNA content and fragmentation (TUNEL assay), area and perimeter of hepatocytes were determined in Feulgen-stained liver imprints. In addition, the activity of aspartate aminotransferase (AST) and alanine aminotransferase (ALT) hepatic transaminases were measured. SedAAS-G1 showed the lowest chromatin condensation and highest Feulgen-DNA content, polyploid nuclei frequency, nuclear area and perimeter, suggesting gene activation. Contrarily, ExAAS-G3 showed a highest chromatin condensation, and a significant decrease of Feulgen-DNA content and decreased frequency of polyploid nuclei, which suggest gene silencing. Image analysis of the nuclear phenotype offered a coherent descriptive picture of the changing patterns of chromatin organization, which were shown to be congruent with the levels of Feulgen-DNA content,

geometric nuclear parameters and hepatocyte activity. In this study, the image analysis permitted the monitoring of the nuclear response to mesterolone and physical exercise action in liver cells, the molecular mechanism of which is in prospect.

**Key words:** Chromatin supraorganization, DNA content, Hepatotoxicity, Image analysis, Mesterolone

## Introduction

Androgenic-anabolic steroids (AAS) are synthetic derivatives of testosterone, which were chemically modified to maximize anabolic and minimize undesirable androgenic effects (Haupt and Rovere, 1984). Pharmacologic and suprapharmacologic doses of AAS and/or testosterone have been successfully used for the treatment of patients with hypogonadism, age-related sarcopenia, HIV-related muscle wasting (Vermeulen, 2001) and protection against ageing-associated decline of cognitive functions (Resnick and Maki, 2001).

During the past few decades, the use of AAS has exceeded the medical recommendations, becoming

**Abbreviations:** AAS, anabolic androgenic steroids or mesterolone; ALT, alanine aminotransferase; Apo-A1, apolipoprotein A1; AST, aspartate aminotransferase; A.U., arbitrary units; CETP, cholesteryl ester transfer protein; Ex, treadmill exercised mice; GA, gum arabic; HDL-C, high-density lipoprotein cholesterol; IOD, integrated optical density; LDL-C, low-density lipoprotein cholesterol; LDL-r, LDL receptor gene; OD, optical density or average absorbance; SDtd, standard deviation of gray average in pixels per nucleus; Sed, sedentary mice; TC, total cholesterol; TG, triglycerides; VLDL, very low density lipoproteins cholesterol.

popular among youth and athletes for their aesthetic body muscle building effects and performance-enhancing properties (Haupt and Rovere, 1984). The abuse of AAS has been associated with the occurrence of premature cardiovascular diseases. These events can negatively be mediated by the appearance of an atherogenic lipoprotein profile which has been associated with AAS self-administration (Taggart et al., 1982; Haffner et al., 1983; Applebaum-Bowden et al., 1987; Glazer, 1991; Hartgens et al., 2004). Besides, epidemiological data have shown the close relationship between AAS use and the high incidence of hepatic disorders, including benign and malignant hepatocellular tumors, cholestatic jaundice, peliosis hepatis, and sub-cellular morphological alterations (Goldman, 1985; Ishak and Zimmerman, 1987; Creagh et al., 1988; Soe et al., 1992; Cabasso, 1994; Kosaka et al., 1996).

Biochemically, the major actions of AAS occur through hormone binding to intracellular receptors in target tissue. This hormone-receptor complex then translocates to chromatin binding sites and binds to its target gene promoter, inducing gene transcription and subsequent synthesis of mRNA (Bahrke and Yesalis, 2004; Wang et al., 2005). The liver expresses estrogen and androgen receptors and experimentally both of those receptors have been implicated in stimulating hepatocyte proliferation, altering the cell cycle, and possibly acting as liver tumor inducers or promoters (Giannitrapani et al., 2006). The increase of lean body mass, muscle size and strength caused by the anabolic effect of AAS results from increased protein metabolism and collagen synthesis (Griggs et al., 1989; Falanga et al., 1999; Bahrke and Yesalis, 2004). It has been reported that dynamic changes to patterns of chromatin condensation are associated with altered cell activity and the cell cycle (Mello and Russo, 1990; Vidal et al., 1998; Leitch, 2000; Maria et al., 2000; Aldrovani et al., 2006; Moraes et al., 2005). Hitherto, a description of accidental alterations provoked by AAS abuse in the chromatin general *status* of cells in the target tissues was not found in current literature.

In a recent study, we showed that the androgenic-anabolic steroid mesterolone caused adverse cardiac remodeling and serious atherogenic lipoprotein profile in sedentary transgenic mice which express the human cholesteryl ester transfer protein (CETP) and are a knockout for the low-density lipoprotein receptor (LDLr) (Fontana et al., 2008). In contrast, in mesterolone administered-treadmill exercised mice, the unfavorable cardiac remodeling and lipoprotein profile was markedly blunted. In this murine transgenic model, the expression of the CETP gene and reduction of the LDL receptor gene (LDLr) expression, drive its lipemic phenotype closer to humans, but apart from the wild type mice which show very low levels of low-density lipoprotein (LDL) and high levels of high-density lipoprotein (HDL) (Cazita et al., 2003; Casquero et al., 2006).

Given the hypothesis that the spatial organization of the interphase nucleus may represent one of the

fundamental control mechanisms in gene expression (Park and De Boni, 1999), the study of nuclear phenotype is an initial step for monitoring transcriptional activity or gene silencing caused by AAS abuse.

This is the first study that utilizes image analysis to investigate the nuclear phenotype of hepatocytes in transgenic CETP<sup>+/-</sup>-LDLr<sup>+/-</sup> mice. The aspect of chromatin supraorganization, DNA content, DNA fragmentation, area and perimeter of hepatocytes nuclei were determined. In addition, aspartate aminotransferase (AST) and alanine aminotransferase (ALT), that are commonly used as markers of inflammation and/or injury, were measured in liver cells homogenate. This is a descriptive study aimed at correlating the alterations of the nuclear phenotype of hepatocyte in transgenic mice, sedentary or submitted to aerobic exercise, to which the anabolic-androgenic steroid mesterolone or gum arabic (vehicle) were administered orally. The utilization of the image analysis method can be prognostic about ongoing transcriptional activities.

## Materials and methods

### Drugs and chemicals

Mesterolone (1alpha-methyl-5alpha-androstan-17beta-ol-3-one) is a non-17 alpha-alkylated derivative of testosterone, whose commercial name is "Proviron", a registered trademark of Schering (Schering do Brazil, São Paulo, SP, Brazil). Gum arabic, also called gum acacia, is taken from *Acacia trees* and purchased from Sigma (St. Louis, MO, USA).

### Animals

The study protocols were approved by the university's Committee for Ethics in Animal Experimentation (CEEA/UNICAMP) and the "Principles of Laboratory Animal Care" (NIH publication no. 85-23, revised 1996) were followed. The transgenic mice used in this study have been cross-bred and maintained in the Department of Physiology and Biophysics, Institute of Biology, UNICAMP for ten years. Mice heterozygous for the human CETP transgene and for LDL-receptor null allele (CETP<sup>+/-</sup>-LDLr<sup>+/-</sup>) have been described elsewhere (Cazita et al., 2003; Casquero et al., 2006). The mice were housed in a temperature-controlled room (22±1°C), humidity of 55-65%, 12h light/dark cycle and had free access to water and standard chow (Nuvilab<sup>®</sup>, Colombo, PR, Brazil).

### Experimental Protocol

Male heterozygous mice (CETP<sup>+/-</sup>-LDLr<sup>+/-</sup>), 2 months old (~22 g body weight) were used. The animals were divided into five groups (n=12/group). Group 1 (G1) – sedentary plus mesterolone (SedAAS); Group 2 (G2) – sedentary plus gum arabic (vehicle) (SedGA); Group 3 (G3) – trained in treadmill plus mesterolone

## AAS vs. nuclear phenotype in hepatocytes of mice

(ExAAS); Group 4 (G4) – trained in treadmill plus vehicle (ExGA); Group 5 (G5) – intact sedentary (blank control) (SedBL). G3 and G4 animals had a week of adaptation, in which a low level of exercise, consisting of treadmill running, was done daily for 5 days (15 m/min during 20 min/day). After the week of adaptation, trained mice were subjected to a 6 weeks of treadmill running, 5 days a week, 60 min/day, as scheduled in Table 1. The animals received mesterolone (AAS) (2 µg/g body weight) or gum arabic (GA) (2 µg/g body weight) by orogastric tube during the last 3 weeks (three days a week: Monday, Wednesday and Friday) of the training or sedentary period (Table 1). In this study, gum arabic was used as vehicle for AAS administration given its proabsorptive effect in the small intestine (Codipilly et al., 2006).

At the end of the experimental period, overnight fasted mice were anesthetized with a 1:1 mixture of ketamine chloride (Dopalen<sup>®</sup>, 100 mg/kg of animal) and xylazine chloride (Anasedan<sup>®</sup>, 10 mg/kg of animal) (2 ml/mg body weight, i.p.). Both anesthetics were purchased from Vetbrands (Jacareí, SP, Brazil). Livers were removed and parts were stored for liver imprints and determination of nuclear phenotype. Other parts of dissected livers were processed for histology, and DNA fragmentation analysis.

### Nuclear phenotypes

Small pieces of liver tissues were dissected out from six animals of each group, placed in cold physiologic solution (0.9% NaCl), and were used to prepare imprints by making direct touch of a surface of the selected livers tissue onto glass slides. The prepared imprints were fixed in a mixture of absolute ethanol – glacial acetic acid (3:1, v/v) for 1 min, rinsed in 70% ethanol for 5 min and then air dried (Moraes et al., 2005).

Imprints were processed according to Feulgen reaction to detect nuclear DNA. Acid hydrolysis was done with 4 M HCl at 25°C for 90 min. Next, the imprints were stained with Schiff's reagent for 40 min, rinsed in sulfurous water (mixture of distilled water, 10% sodium metabisulfite and 1 M HCl; 18:1:1; v/v/v) and distilled water, air-dried, cleared in xylene and mounted with a coverslip in natural Canada balsam (nD=1.54) (Vetec, Rio de Janeiro, RJ, Brazil). Nuclei stained with the Feulgen reaction were analyzed using Olympus microscopy (Olympus American Inc., NY, USA) equipped with 40x UplanFl objective, optovar 2, 0.90 condenser and 546 nm wavelength. The images were captured using a Q-color 3 digital video camera (Olympus American Inc., NY, USA), transmitted to a Pentium 4 computer and analyzed using Image-Pro-Plus 5.01 software for Windows (Media Cybernetics, Inc., NY, USA). The parameters analyzed were optical density (OD = average absorbance), standard deviation of gray average in pixels per nucleus (SDtd of OD), Feulgen-DNA values (integrated optical density, IOD, in arbitrary units, A.U.), nuclear area (µm<sup>2</sup>) and nuclear

perimeter (µm). For each of the experimental groups 460 hepatocytes nuclei were analyzed. Fifty (50) nuclei of lymphocytes from the blank control (SedBL-G5) group were also analyzed as reference for establishing the classes of hepatocytes ploidy (Feulgen-DNA values), given lymphocytes typical diploid standard 2C-DNA content (Hayday et al., 1985).

### DNA fragmentation

After sacrifice of the mice and removal of the liver, some pieces of tissue were destined for examination of DNA fragmentation associated with programmed cell death. Fragments of livers of the five groups (n = 6 animals/group) were fixed in 4% paraformaldehyde and embedded in paraffin. Sections 5 µm thick were dewaxed, submitted to a descendent ethanol series and washed in distilled water to examine DNA fragmentation using the TUNEL POD assay, as described by the manufacturer (Roche/Amersham). Since UTP was labeled with fluorescein, anti-fluorescein antibodies coupled to peroxidase were incubated with 3-3'-diaminobenzidine (DAB, Sigma Chemical, St. Louis, MO, USA) for 10 min at room temperature (25°C). Counter-staining was done with hematoxylin (Merck KGaA, Darmstadt, Germany), followed by rinsing in distilled water. The preparations were then air dried and mounted in natural Canada balsam. Endogenous peroxidase was blocked with 3% H<sub>2</sub>O<sub>2</sub> in absolute methanol for 30 min at room temperature. A negative control was done by excluding the TdT enzyme from the reaction. As positive controls, preparations incubated with DNase I (3000 U/mL in 50 mM Tris-HCl, pH 7.5, 10 mM MgCl<sub>2</sub> 1 mg/mL BSA, for 10 min at 25°C) were also used.

### Measurement of enzymatic activity

At the end of the experimental protocol, all mouse groups (n=6) were anesthetized as described above, and the livers were removed, rinsed repeatedly with large volumes of physiological saline, and homogenized by hand in five volumes of ice-cold 0.1 M potassium phosphate buffer, pH 7.4, containing 0.15 M KCl and 1 mM EDTA, and the crude homogenate was centrifuged

**Table 1.** Exercise (6 weeks) and AAS or vehicle administration (3 weeks) protocol.

Weeks	Velocity (m/min)	Duration (min)
1	12.42	20
2	14.70	30
3	16.68	45
4 - 6 (*)	17.04	60

(\*) AAS or gum arabic (vehicle) administered orally by gavage at 10:00 a.m. (Monday, Wednesday and Friday) in the last three weeks.

at 9000g for 20 min. Ultracentrifugation to pellet the microsomal fraction was performed at 105 000g for 1 h. Supernatant was stored as cytosolic fraction. All procedures were carried out at 0-4°C. The activities of glutamic oxalacetic transaminase (GOT - AST) and glutamic-pyruvic transaminase (GPT - ALT) were measured in the supernatant of homogenized livers according to the instructions of the manufacturer contained in commercially available kits (Laborlab no 02600, Guarulhos, SP, Brazil).

### Statistical analysis

All calculations and statistical analyses were done using the Minitab 12™ software (State College, PA, USA) and involved frequency histograms, marginal and regression plots, sort manipulation and Analysis of Variance (Anova), Kruskal-Wallis and Mann-Whitney post-tests. Differences were considered statistically significant at P-values < 0.05.

## Results

### Nuclear phenotypes

Color digital images of Feulgen-positive hepatocyte nuclei were converted for gray levels and used for establishing nuclear phenotypes. After the conversion, nuclei of the population of each mouse group showed variations in the level of gray intensity, reflecting differences in chromatin packaging, and chromocenters (areas of more condensed chromatin). Only a digital image of the control sample is displayed (Fig. 1A) because differences of nuclear phenotypes among the groups studied can only be discernible by computer-aided image analysis, and not visually. Fig. 1B displays hepatocyte nuclei after image treatment that allows us to visualize in detail areas of more condensed chromatin/chromocenters.

Image analysis of preparations stained with Feulgen reaction yielded the values listed in Tables 2 and 3.

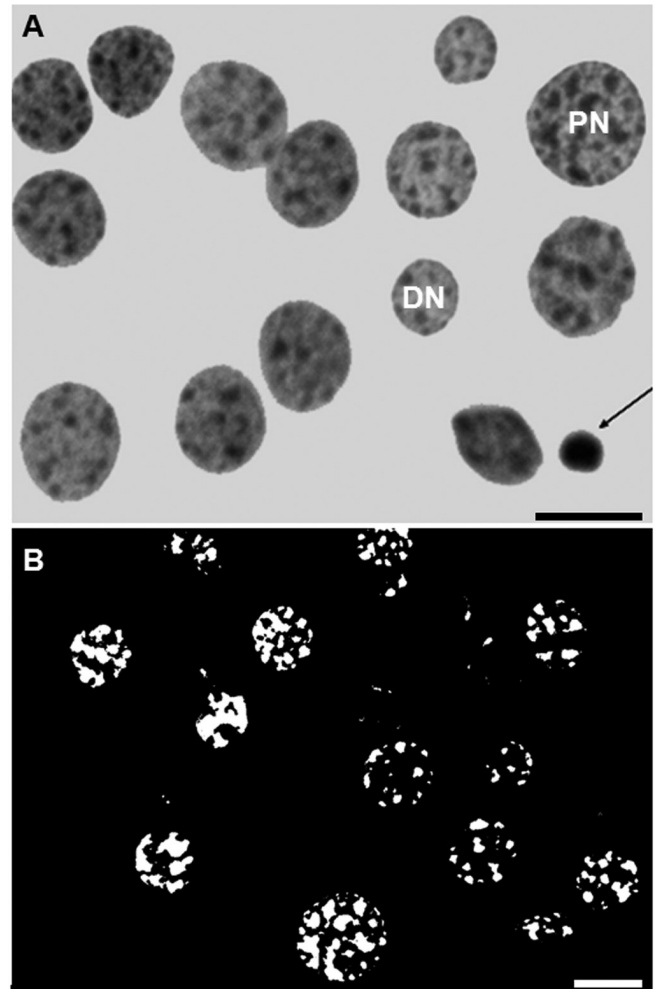


**Fig. 1.** A. Digital image of blank hepatocyte nuclei stained with the Feulgen reaction. The image was converted for the gray levels using Image-Pro-Plus software. PN, polyloid nucleus; DN, diploid nucleus. The arrow indicates a lymphocyte that was used as control for ploidy. B. Hepatocyte nuclei after image treatment for visualization of more condensed chromatin/chromocenters. Bars: 1.25  $\mu$ m.

**Table 2.** Evaluation of densitometric and textural parameters by image analysis of Feulgen-stained hepatocyte nuclei obtained from liver imprints of CETP<sup>+/+</sup>/LDLR<sup>+/+</sup> transgenic mice.

Experimental groups	IOD		OD		SDtd	
	$\eta$	Z	$\eta$	Z	$\eta$	Z
G1-Sedentary treated with mesterolone	37.28 <sup>a</sup>	6.82	0.3082 <sup>a</sup>	-16.14	0.0380 <sup>a</sup>	-23.14
G2-Sedentary treated with gum arabic	32.00 <sup>c</sup>	-2.53	0.3902 <sup>b</sup>	-2.90	0.0799	8.76
G3-Trained treated with mesterolone	34.51 <sup>e</sup>	0.46	0.4157 <sup>c</sup>	19.22	0.0959	20.07
G4-Trained treated with gum arabic	20.82 <sup>d</sup>	-11.19	0.3324	-11.72	0.0904	15.61
G5-Control (intact sedentary)	36.00 <sup>b</sup>	6.45	0.3389 <sup>d</sup>	-2.35	0.0432 <sup>b</sup>	-21.30

Statistical tests, Kruskal-Wallis;  $\eta$ , median; Z-value, indicates how the mean rank for each group differs from the mean rank for all groups; IOD, integrated optical density (Feulgen-DNA values); OD, optical density (absorbance); SDtd, standard deviation of the gray average, in pixels, per nucleus; number of measurements, 460. All comparing values show significant statistical difference (p<0.05) IOD: G1 (a) vs. G5 (b); G2 (c) vs. G5 (b); G3 (e) vs. G5 (b); G4 (d) vs. G5 (b); OD: G1 (a) vs. G2 (b); G2 (b) vs. G3 (c); G1 (a) vs. G5 (d); SDtd: G1 (a) vs. G5 (b).

*AAS vs. nuclear phenotype in hepatocytes of mice*

**Table 3.** Evaluation of geometric parameters by image analysis of Feulgen-stained hepatocyte nuclei obtained from liver imprints of CETP<sup>+/+</sup>/LDL<sup>r+/+</sup> transgenic mice.

Experimental groups	Area		Perimeter	
	$\eta$	Z	$\eta$	Z
G1-Sedentary treated with mesterolone	122.45	16.98	44.7 a	12.33
G2-Sedentary treated with gum arabic	75.23	2.41	34.39	- 6.96
G3-Trained treated with mesterolone	75.63	1.96	34.66 c	- 8.81
G4-Trained treated with gum arabic	71.66	3.28	35.46 d	- 3.80
G5-Control (intact sedentary)	99.85	11.62	41.24 b	7.24

Statistical tests, Kruskal-Wallis; $\eta$ , arithmetic median; Z-value, indicates how the mean rank for each group differs from the mean rank for all groups; number of measurements, 460. All comparing values show significant statistical difference ( $p < 0.05$ ). Perimeter: G1 (a) vs. G5 (b); G3 (c) vs. G4 (d).

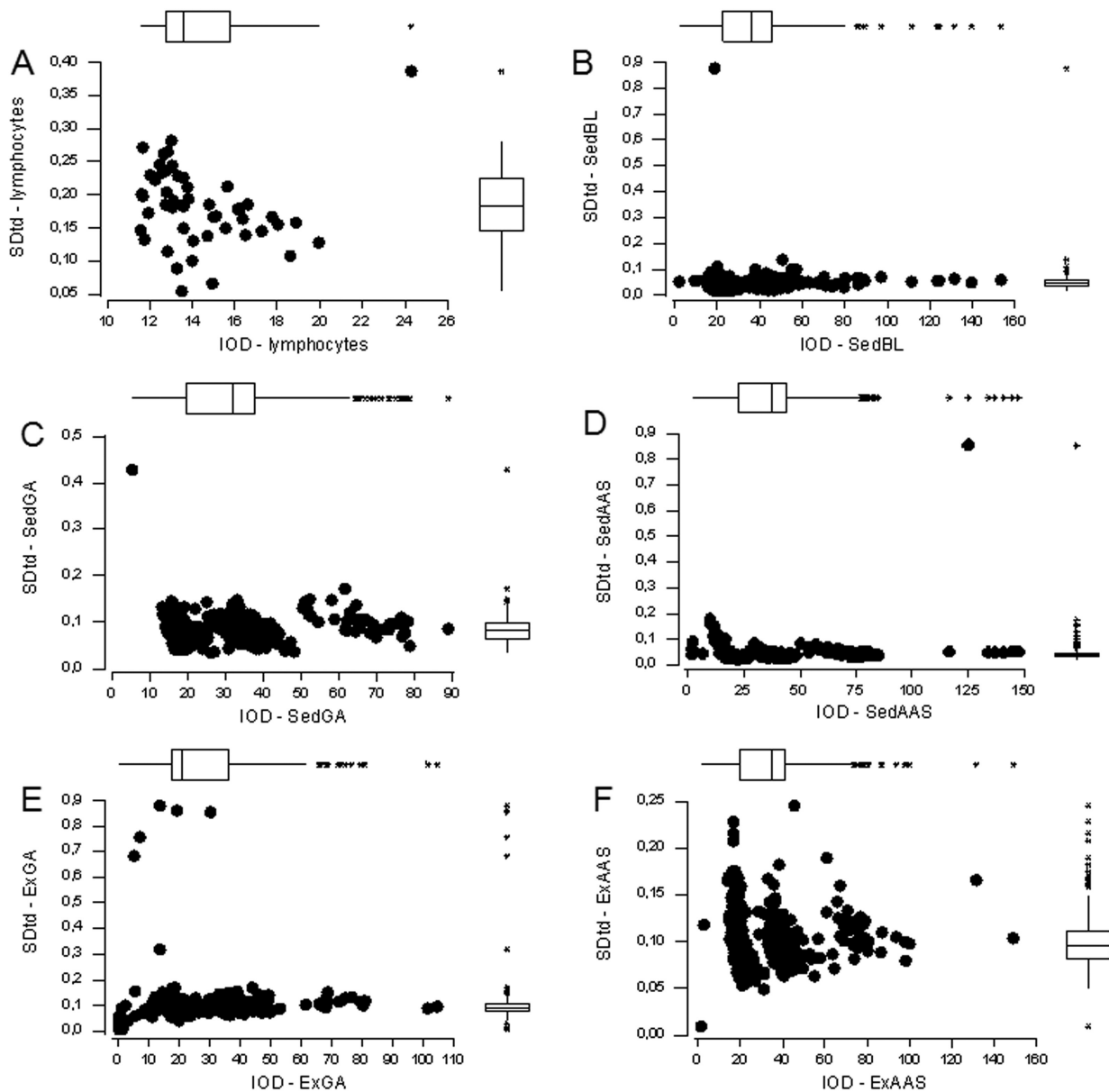


**Fig. 2.** Marginal plot of SDtd in function of IOD. SedBL, sedentary blank controls; SedGA, sedentary plus gum arabic; SedAAS, sedentary plus mesterolone; ExGA, trained in treadmill plus gum arabic; ExAAS, trained in treadmill plus mesterolone.

*AAS vs. nuclear phenotype in hepatocytes of mice*

Hepatocyte nuclei from sedentary animals treated with mesterolone (SedAAS-G1) showed the lowest values of OD (chromatin condensation for nuclei populations) and SDtd (chromatin diffuseness index per individual nuclei) compared to the other mice groups (Table 2). In contrast,

ExAAS-G3 showed the highest OD and SDtd values. No significant difference was observed between SDtd values of ExAAS-G3 and ExGA-G4 groups ( $P < 0.05$  level). OD and SDtd are correlated by the fact that the nuclei image is saved in bytes containing the total values of the gray

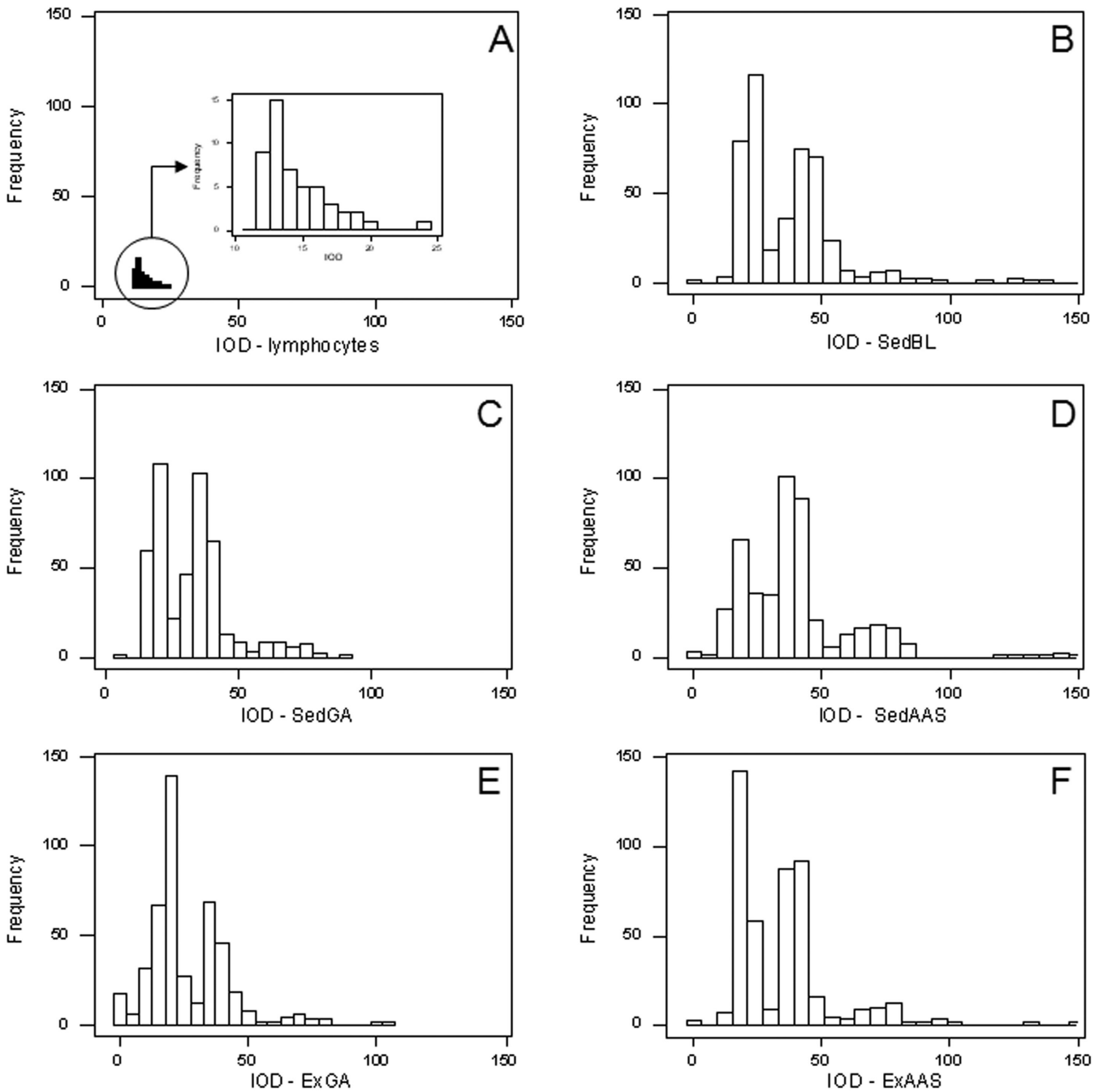


**Fig. 3.** Frequency histograms of the Feulgen-DNA values obtained for the mice groups studied. IOD values from hepatocytes were compared to IOD values obtained from lymphocytes, which typically showed a single peak indicating that the content of DNA is 2C. SedBL, sedentary blank controls; SedGA, sedentary plus gum arabic; SedAAS, sedentary plus mesterolone; ExGA, trained in treadmill plus gum arabic; ExAAS, trained in treadmill plus mesterolone.

AAS vs. nuclear phenotype in hepatocytes of mice

intensity levels that are transformed in OD.

Graphics of SDtd in function of IOD (IOD is calculated as OD x nuclear area, and OD is correlated with SDtd as previously mentioned) were constructed (Fig. 2), showing that the nuclei with the highest IOD values possess the smallest contrast between condensed and descondensed chromatin (SDtd values). All experimental groups, except SedAAS-G1, presented higher spreading of IOD and SDtd values than intact sedentary SedBL-G5. The ExAAS-G3 group displayed the highest spreading of SDtd values (Fig. 2F).

IOD median values, listed in Table 2, show the Feulgen-DNA content. All mice groups, except SedAAS-G1 which showed the highest value, showed hepatocyte nuclei with lower IOD values than the intact sedentary SedBL-G5 group. The lowest IOD median value was observed in treadmill trained gum arabic-treated animals (ExGA-G4), followed by sedentary gum

arabic-treated mice (SedGA-G2) and treadmill trained mesterolone-treated mice (ExAAS-G3), respectively. Significant differences were observed between IOD median values from hepatocyte nuclei of all groups in comparison with the blank control mice (SedBL-G5), including SedAAS-G1 vs. SedBL-G5 ( $P_{0.02}$  level).

The distribution of the hepatocytes' IOD values was analyzed by frequency histograms to show levels of ploidy. IOD values from hepatocyte nuclei were established by comparison with IOD values from lymphocyte nuclei, which typically showed a single peak relative to 2C-DNA content or diploid nuclei. Lymphocyte IOD values were distributed in the interval of 11.5–25 A.U. (Fig. 3A), indicating that these Feulgen-DNA values represent diploid nuclei in different phases of the cell cycle. Hepatocytes from all groups (G1 to G5) showed multimodal distribution of the IOD values (Fig. 3 B-F), indicating the presence of nuclei with different

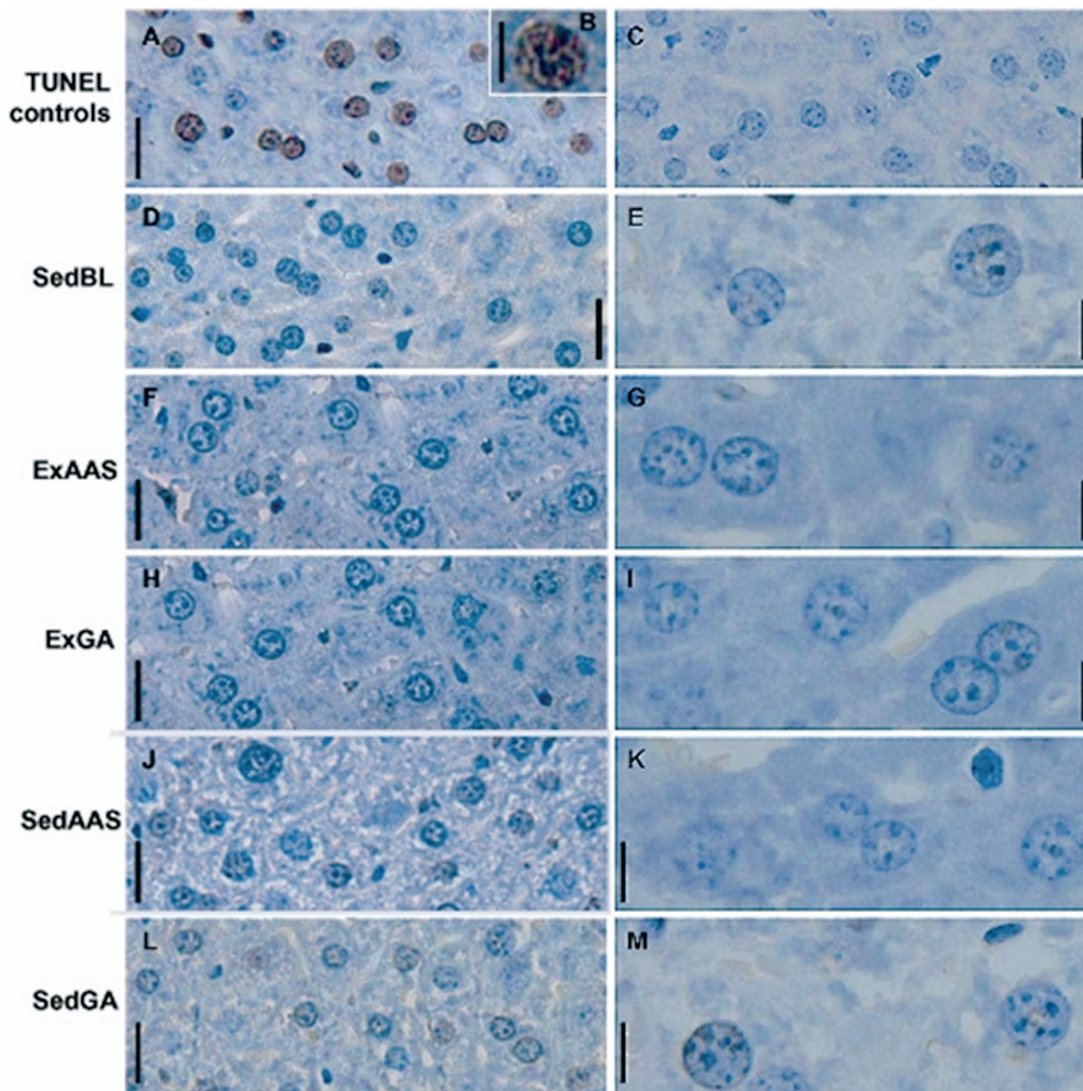


**Fig. 4.** Hepatocyte nuclei subjected to the TUNEL assay. **A and B**, hepatocytes subject to treatment with DNaseI (positive controls); **C**, negative control; **D and E**, Sedentary blank controls (SedBL); **F and G**, trained in treadmill plus mesterolone (ExAAS); **H and I**, trained in treadmill plus gum arabic (ExGA); **J and K**, sedentary plus mesterolone (SedAAS); **L and M**, sedentary plus gum arabic (SedGA). Bars: A, C, D, F, H, J, L, 25  $\mu$ m; B, E, G, I, K, M, 10  $\mu$ m.

## AAS vs. nuclear phenotype in hepatocytes of mice

ploidy levels. Those with IOD values between 11.5–25 A.U. were diploids, whereas those with IOD  $\geq 25.1$  A.U. were polyploids (25.1–50 A.U. = 4C-DNA, 50–99.9 A.U. = 8C-DNA and  $\geq 100$  = 16C-DNA content). A sort manipulation (Minitab 12™ software) of the IOD values allowed us to calculate the number of polyploid nuclei present in each hepatocyte population studied ( $n = 460$ ): nuclei with IOD values  $\geq 25.1$  A.U. (polyploids) were 330 in SedAAS-G1; 271 in SedGA-G2; 297 in ExAAS-G3; 184 in ExGA-G4; and 309 in SedBL-G5. Interestingly, all hepatocyte populations showed some nuclei with smaller IOD values than the minimum value obtained for lymphocytes (11.5 A.U.). Nuclei with IOD values  $< 11.5$  A.U. was for G1= 6; G2= 1; G3= 2; G4= 34; and G5= 3 nuclei.

Hepatocyte nuclei from sedentary mice treated with mesterolone (SedAAS-G1) showed higher values for geometric parameters (nuclear area and perimeter) in comparison to hepatocyte nuclei of all other groups. The values of nuclear area and perimeter obtained for each sample are displayed in the Table 3.

The correlations between nuclear areas and Feulgen-DNA values were obtained using Minitab 12™ software and were expressed as a quadratic linear regression ( $R^2$ ). For all mice groups, except ExAAS-G3, there were no significant differences in the correlation coefficients when compared to the intact sedentary SedBL-G5 group (Table 4).

### DNA fragmentation

DNA fragmentation typical of programmed cell death and/or apoptosis was not detected by the TUNEL assay in the hepatocytes studied (Fig. 4D-M) and in the negative controls (Fig. 4C); a positive response was obtained in hepatocytes incubated with DNase I (Fig. 4A, B).

### Transaminases

AST and ALT activities were detected in all samples, determined six weeks after beginning the experiments, and showed no significant difference among the groups studied ( $P > 0.05$ ) (Fig. 5). However,

**Table 4.** Correlation coefficient ( $R^2$ ), in percentage, between nuclear area and Feulgen-DNA content (integrated optical density, IOD).

Mice	$R^2$ (%)
G1- Sedentary treated with androgenic	64.5
G2-Sedentary treated with gum arabic	81.8
G3-Trained treated with androgenic	87.4
G4-Trained treated with gum arabic	83.2
G5-Control (intact sedentary)	90.1

For all mice groups, except G3, there were no significant differences in correlation coefficients when compared to the intact sedentary G5 group. ( $P < 0.05$ ): G1 VS. G5; G2 VS. G5; G4 VS. G5.

there was a trend to increase AST in SedAAS, with exercise counteracting this effect (see ExAAS).

### Discussion

The indiscriminate self-administration of anabolic-androgenic steroids has been associated with relevant hepatocellular disorders and development of an atherogenic profile in drug abusers (Goldman, 1985, Ishak and Zimmerman, 1987; Creagh et al., 1988; Soe et al., 1992; Cabasso, 1994; Kosaka et al., 1996). Herein, the computer-aided image analysis of the state of chromatin supraorganization, texture, DNA content/fragmentation, and geometric parameters in interphase nucleus of hepatocytes in intact, sedentary or exercised CETP<sup>+/-</sup>/LDLr<sup>+/-</sup> transgenic mice treated with mesterolone or vehicle showed interesting differences. This heterozygous transgenic mouse has a lipemic profile akin to humans, and as such, is useful for studies aiming to reproduce clinical research. Hepatic CETP mediates the plasma cholesteryl ester transfer from high-density lipoprotein (HDL) to apolipoprotein B (apoB)-containing lipoproteins (very low-density lipoprotein (VLDL) and low-density lipoprotein (LDL) in exchange

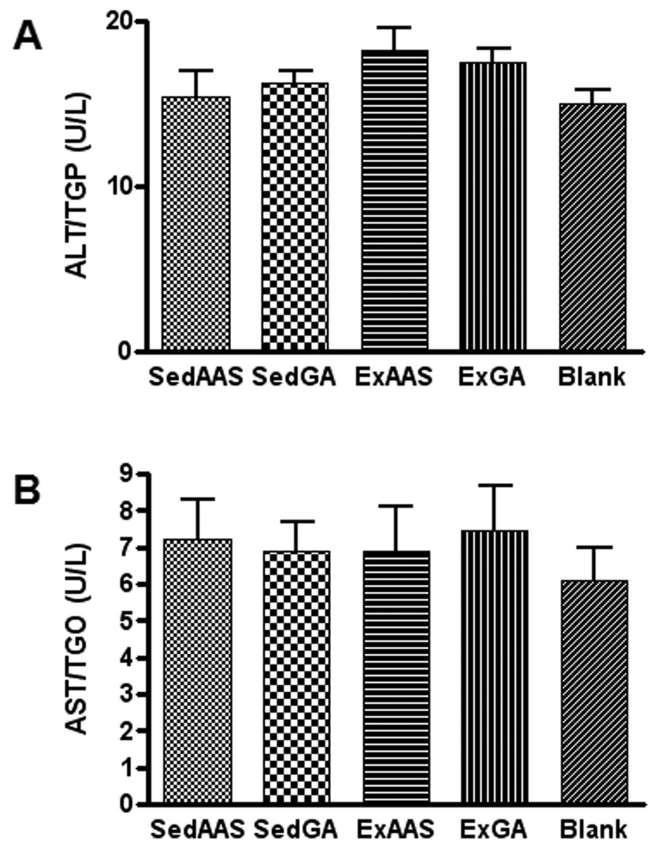


**Fig. 5.** AST and ALT activities measured in the supernatant of homogenized livers.

## AAS vs. nuclear phenotype in hepatocytes of mice

for triacylglycerol (Bruce et al., 1998). In humans, CETP mRNA is predominantly expressed in the liver and is secreted by hepatocytes. An increase in plasma CETP and hepatic CETP mRNA in transgenic mice expressing the human CETP gene can be induced by environmental conditions, such as alcohol, smoking, obesity, dietary alterations and drugs such as cholestyramine and statins (Jiang et al., 1992; Harada et al., 2006).

In our murine model, the six weeks of exercise (5 times/week) and the three weeks of mesterolone oral administration represent a considerable time-interval in terms of duration/intensity of the physical exercise, and period of drug abuse in human life cycle (Bronson and Matherne, 1997). Hence, this model can be useful for studies of complications of anabolic steroid misuse.

The present results showed that the lowest absorbance values (OD) were observed in sedentary mice treated with mesterolone (SedAAS-G1), and were compatible with chromatin unpacking. In addition, this was substantiated by the least contrast between the higher and lower packaging states of chromatin (SDtd) found in the same group. Recent study in our laboratory with this lipemic mice strain, and using the same protocol as for the present study, showed that sedentary animals treated with mesterolone (SedAAS-G1) was the group which presented the highest plasmatic levels of total cholesterol (TC), triglycerides (TG), low-density lipoprotein (LDL) and very low-density lipoproteins (VLDL), while high-density lipoprotein (HDL) levels were slightly below that of SedGA (Fontana et al., 2008). A simultaneous decrease in OD and SDtd values in hepatocyte nuclei has been associated with the recovery of transcriptional activities after refeeding of a 48 h-fasted inbred strain A/Uni mice (Cassia et al., 1991; Moraes et al., 2005). In contrast, the highest spreading of IOD (OD x area) and SDtd values observed in ExAAS-G3 is both an indication of increased packaging of certain chromatin areas, as well as of increased contrast between condensed and uncondensed chromatin. Since in exercised-vehicle mice (ExGA-G4) the level of chromatin condensation was higher than in SedAAS, but lower than in ExAAS, such chromatin remodeling may show that physical exercise counteracted the effects of AAS. The opponent (modulatory) action of exercise against mesterolone was also seen in the lipoprotein profile (Fontana et al., 2008). ExAAS showed a significant decrease of TG, LDL and VLDL, and more importantly, an increase of HDL in relation to SedAAS-G1. The lowering in plasmatic levels of lipid and lipoproteins in ExAAS is in agreement with the highest OD (chromatin condensation) and SDtd (chromatin diffuseness) values obtained for the group. Taken together, the chromatin remodeling seen by image analysis suggest an upregulation of transcriptional activity in SedAAS-G1 and a synthesis inhibition of some lipoproteins in ExAAS, or an antagonistic effect of mesterolone vs. exercise. However, it could not be ignored that the control of DNA condensation is mediated via protein-chromatin interactions and

influenced by epigenetic phenomena such as DNA methylation (Keshet et al., 1986) and histone acetylation (Houben et al., 1996). These epigenetic factors may be involved with transcriptional activity or gene silencing as suggested by the nuclear phenotype of hepatocytes in the current study. There are much molecular evidences to suggest that AAS acts by activating genes related with the synthesis of liver enzymes (Labrie et al., 2005). In the present study, it is possible that genes involved with lipid metabolism could have been also affected. However, we did not find differences in plasmatic levels of liver transaminases AST and ALT. There was not a consensus about transaminases changes due to AAS use in pertinent literature (see Glazer, 1991 for a review), and this could be attributed to differences in protocol, the kind of AAS and the animal studied.

In accordance with the results of OD and SDtd, the median values of IOD (Feulgen-DNA content) corroborate the hypothesis of highest gene activity in sedentary mice treated with mesterolone (SedAAS-G1). The G1-group showed the highest elevation of the Feulgen-DNA content in relation to all other groups, including the blank control mice (SedBL-G5). Note that nuclei with the highest IOD values were shown to possess the smallest contrast between condensed and uncondensed chromatin (SDtd values). It was also the SedAAS-G1 group which exhibited the highest perimeter and area of the interphase nucleus. This was positively correlated with the higher Feulgen-DNA content measured in SedAAS.

One phenomenon that can explain the present results is the polyploidization. The increase in IOD values triggered by AAS administration to sedentary mice (SedAAS-G1-group) is apparently associated with the highest frequency of polyploid nuclei in the G1 hepatocytes population. This would also be responsible for the larger values of the geometric parameters (nuclear area and perimeter) detected for the nuclei of the G1-group. Seventy percent of the G1 nuclei were polyploids. The hypothesis is feasible since there was a strict positive correlation between IOD median values and geometric nuclei parameters, with values indicating  $G1 > G5 > G3 > G2 > G4$  (in which decreased nuclear area and perimeter are in conformity with the smaller Feulgen-DNA content), and the percentage of polyploids nuclei, where  $(G1 = 330:70\%) > (G5 = 309:67\%) > (G3 = 297:64\%) > (G2 = 271:58\%) > (G4 = 184:40\%)$ . Polyploidy results from incomplete mitotic cycles, and are generally related to increased physiological demands (Nicolini, 1980; Aldrovani et al., 2006). On other the hand, in terms of relative diploid hepatocytes frequency the results showed  $G4 > G2 > G3$  groups, which was inversely proportional to IOD median values, i.e.,  $G4 < G2 < G3$ . Another fact to be considered was that hepatocyte nuclei showing smaller IOD values than lymphocytes (11.5 A.U.) were observed in all groups studied. This may be indicative of a certain degree of DNA fragmentation and loss, as happens in apoptosis or programmed cell death (Maria et al., 2000), or due to

DNA hydrolysis during processing. We believe that the DNA/apurinic acid fragmentation is the most plausible explanation in the present case, since no positive response to the TUNEL assay has been revealed in the hepatocytes studied.

In conclusion, the present study is pioneering in demonstrating that the chronic use of mesterolone affects dynamically the status of chromatin condensation and texture, geometric parameters and Feulgen-DNA values in hepatocyte nuclei of sedentary and trained mice. Mesterolone induced in sedentary mice the highest Feulgen-DNA content, which we credited both to the higher number of polyploidy cells and unpackaging of the chromatin associated to the highest increase of the nuclear size. The assessment of nuclear phenotype by image analysis can give clues to the mechanisms underlying the effects of AAS and its interplay with exercise effects in transcriptional activation or repression of eukaryotic genes. This study using a human-like lipemic mouse strain is part of a comprehensive study aimed to further understand the effects of AAS abuse. We believe that this study will allow us to continue investigations to understand the mechanisms by which gene alterations and/or epigenetic factors provoked by the use of AAS may be linked with hepatocellular dysfunction.

---

*Acknowledgements.* This study was supported by grants from Fundação de Amparo à Pesquisa do Estado de São Paulo (FAPESP) (Proc. 04/13767-9 and 03/04597-0) and Conselho Nacional de Desenvolvimento Científico e Tecnológico (CNPq) (Proc. 522131/95-6 and 0410/2003-0). K.F. is a PhD student granted with a scholarship from FAPESP (Proc. 04/13768-5); B.C.V. and M.A.C.H. are supported by research fellowships from the Conselho Nacional de Desenvolvimento Científico e Tecnológico (CNPq). The authors thank Mrs. Marta B. Leonardo for technical assistance. There is no conflict of interest that would prejudice the impartiality of this research.

---

## References

- Aldrovani M., Mello M.L.S., Guaraldo A.M.A. and Vidal B.C. (2006). Nuclear phenotypes and DNA fragmentation in tendon fibroblasts of NOD mice. *Caryologia* 59, 116-124.
- Applebaum-Bowden D., Haffner S.M. and Hazzard W.R. (1987). The dyslipoproteinemia of anabolic steroid therapy: increase in hepatic triglyceride lipase precedes the decrease in high density lipoprotein2 cholesterol. *Metabolism* 36, 949-952.
- Bahrke M.S. and Yesalis C.E. (2004). Abuse of anabolic androgenic steroids and related substances in sports and exercise. *Curr. Opin. Pharmacol.* 6, 614-620.
- Bronson F.H. and Matherne C.M. (1997). Exposure to anabolic-androgenic steroids shortens life span of male mice. *Med. Sci. Sports Exerc.* 29, 615-619.
- Bruce C., Chouinard Jr R.A. and Tall A.R. (1998). Plasma lipid transfer proteins, high-density lipoproteins, and reverse cholesterol transport. *Annu. Rev. Nutr.* 18, 297-330.
- Cabasso A. (1994). Peliosis hepatic in a young adult bodybuilder. *Med. Sci. Sports Exerc.* 26, 2-4.
- Casquero A.C., Berti J.A., Salerno A.G., Bighetti E.J., Cazita P.M., Ketelhuth D.F., Gidlund M. and Oliveira H.C. (2006). Atherosclerosis is enhanced by testosterone deficiency and attenuated by CETP expression in transgenic mice. *J. Lipid Res.* 47, 1526-1534.
- Cassia R.O., Pucciarelli M.G. and Conde R.D. (1991). Effect of dietary level of protein on the metabolism of mouse liver nuclear proteins. *Horm. Metab. Res.* 23, 585-589.
- Cazita P.M., Berti J.A., Aoki C., Gidlund M., Harada L.M., Nunes V.S., Quintao E.C. and Oliveira H.C. (2003). Cholesteryl ester transfer protein expression attenuates atherosclerosis in ovariectomized mice. *J. Lipid Res.* 44, 33-40.
- Codipilly C.N., Teichberg S. and Wapnir R.A. (2006). Enhancement of absorption by gum arabic in a model of gastrointestinal dysfunction. *J. Am. Coll. Nutr.* 25, 307-312.
- Creagh T.M., Rubin A. and Evans D.J. (1988). Hepatic tumors induced by anabolic steroid in an athlete. *J. Clin. Pathol.* 41, 441-443.
- Falanga V., Greenberg A.S., Zhou L., Ochoa S.M., Roberts A.B., Falabella A. and Yamaguchi Y. (1999). Stimulation of collagen synthesis by the anabolic steroid stanozolol. *J. Invest. Dermatol.* 111, 1193-1197.
- Fontana K., Oliveira H.C.F., Leonardo M.B., Mandarim-de-Lacerda C.A., Cruz-Höfling M.A. (2008). Adverse effect of anabolic androgenic steroid mesterolone on cardiac remodeling and lipoprotein profile is attenuated by aerobic exercise training. *Int. J. Exp. Pathol.* (in press).
- Giannitrapani L., Soresi M., La Spada E., Cervello M., D'Alessandro N. and Montalto G. (2006). Sex hormones and risk of liver tumor. *Ann. NY Acad. Sci.* 1089, 228-236.
- Glazer G. (1991). Atherogenic effects of anabolic steroids on serum lipid levels. A literature review. *Arch. Intern. Med.* 151, 1925-1933.
- Goldman B. (1985). Liver carcinoma in an athlete taking anabolic steroid [letter]. *J. Am. Osteopath. Assoc.* 85, 56.
- Griggs R.C., Kingston W., Jozefowicz R.F., Herr B.E., Forbes G. and Halliday D. (1989). Effect of testosterone on muscle mass and muscle protein synthesis. *J. Appl. Physiol.* 66, 498-503.
- Haffner S.M., Kushwaha R.S., Foster D.M., Applebaum-Bowden D. and Hazzard W.R. (1983). Studies on the metabolic mechanism of reduced high density lipoproteins during anabolic steroid therapy. *Metabolism* 32, 413-420.
- Harada L.M., Carrilho A.J., Oliveira H.C., Nakandakare E.R. and Quintao E.C. (2006). Regulation of hepatic cholesterol metabolism in CETP/LDLr mice by cholesterol feeding and by drugs (cholestyramine and lovastatin) that lower plasma cholesterol. *Clin. Exp. Pharmacol. Physiol.* 33, 1209-1215.
- Hartgens F., Rietjens G., Keiser H.A., Kuipers H. and Wolffenbuttel B.H. (2004). Effects of androgenic-anabolic steroids on apolipoproteins and lipoprotein (a). *Br. J. Sports Med.* 38, 253-259.
- Haupt H.A. and Rovere G.D. (1984). Anabolic steroids: a review of the literature. *Am. J. Sports Med.* 12, 469-484.
- Hayday A.C., Saito H., Gillies S.D., Karnaz D.M., Tanigawa G., Eisen H.N. and Tonegawa S. (1985). Structure, organization, and somatic rearrangement of T cell gamma genes. *Cell* 40, 259-269.
- Houben A., Belyaev N.D., Turner B.M. and Schubert I. (1996). Differential immunostaining of plant chromosomes by antibodies, recognising acetylated histone H4 variants. *Chromosome Res.* 4, 191-195.
- Ishak K.G. and Zimmerman H.J. (1987). Hepatotoxic effects of the anabolic/androgenic steroids. *Semin. Liver Dis.* 7, 230-236.
- Jiang X.C., Agellon L.B., Walsh A., Breslow J.L. and Tall A. (1992).

*AAS vs. nuclear phenotype in hepatocytes of mice*

- Dietary cholesterol increases transcription of the human cholesteryl ester transfer protein gene in transgenic mice. *J. Clin. Invest.* 90, 1290-1295.
- Keshet I., Yisraeli J. and Cedar H. (1986). DNA methylation affects the formation of active chromatin. *Cell* 44, 535-543.
- Kosaka A., Takahashi H., Yajima Y., Tanaka M., Okamura K., Mizumoto R. and Katsuta K. (1996). Hepatocellular carcinoma associated with anabolic steroid therapy: report of a case and review of the Japanese literature. *J. Gastroenterol.* 31, 450-454.
- Labrie F., Luu-The V., Calvo E., Martel C., Cloutier J., Gauthier S., Belleau P., Morissette J., Levesque M.H. and Labrie C. (2005). Tetrahydrogestrinone induces a genomic signature typical of a potent anabolic steroid. *J. Endocrinol.* 184, 427-433.
- Leitch A.R. (2000). Higher levels of organization in the interphase nucleus of cycling and differentiated cells. *Microbiol. Mol. Biol. Rev.* 64, 138-152.
- Maria S.S., Vidal B.C. and Mello M.L.S. (2000). Image analysis of DNA fragmentation and loss in V79 cells under apoptosis. *Genet. Molec. Biol.* 23, 109-112.
- Mello M.L.S. and Russo J. (1990). Image analysis of Feulgen-stained c-H-ras transformed NIH/3T3 cells. *Biochem. Cell Biol.* 68, 1026-1031.
- Moraes A.S., Vidal B.C., Guaraldo A.M.A. and Mello M.L.S. (2005). Chromatin supraorganization and extensibility in mouse hepatocyte following starvation and refeeding. *Cytometry* 63, 94-107.
- Nicolini C. (1980). Nuclear morphology, quaternary chromatin structure and cell growth. *J. Submicr. Cytol.* 12, 475-505.
- Park P.C. and De Boni U. (1999). Dynamics of structure-function relationships in interphase nuclei. *Life Sci.* 64, 1703-1718.
- Resnick S.M. and Maki P.M. (2001). Effects of hormone replacement therapy on cognitive and brain aging. *Ann. NY Acad. Sci.* 949, 203-214.
- Soe K.L., Soe M. and Gluud C. (1992). Liver pathology associated with the use of anabolic-androgenic steroids. *Liver* 12, 73-79.
- Taggart H.M., Applebaum-Bowden D., Haffner S., Warnick G.R., Cheung M.C., Albers J.J., Chestnut C.H. 3rd and Hazzard W.R. (1982). Reduction in high density lipoprotein by anabolic steroid (stanozolol) therapy for postmenopausal osteoporosis. *Metabolism* 31, 1147-1152.
- Vermeulen A. (2001). Androgen replacement therapy in the aging male: a critical evaluation. *J. Clin. Endocrinol. Metab.* 86, 2380-2385.
- Vidal B.C., Russo J. and Mello M.L. (1998). DNA content and chromatin texture of benzo[a]pyrene-transformed human breast epithelial cells as assessed by image analysis. *Exp. Cell. Res.* 244, 77-82.
- Wang L., Hsu C.L. and Chang C. (2005). Androgen receptor co-repressors: an overview. *Prostate* 63, 117-130.

Accepted June 9, 2008